

## ELECTRONIC STRUCTURES OF TRIS(CYCLOPENTADIENYL)URANIUM(IV)-LIGAND COMPLEXES \*

KAZUYUKI TATSUMI and AKIRA NAKAMURA\*

*Department of Macromolecular Science, Faculty of Science, Osaka University, Toyonaka, Osaka 560 (Japan)*

(Received May 18th, 1984)

### Summary

We present a systematic molecular orbital study of the electronic and geometrical structure of complexes containing the  $\text{Cp}_3\text{U}$  fragment bonded to a variety of organic ligands. Nature of U–C bonding is variegated, as is incarnated in a remarkable range of U–C distances. As measured by overlap populations, covalency in the U–C(alkyl)  $\sigma$  bond is strong, but very weak in the case of the U–Cp  $\pi$  bond. Covalency in the U–CHPR<sub>3</sub> and U–CCR bonds is even enhanced due to additional interactions, more for the former, indicating the presence of partial multiple bond character.

---

### Introduction

In modern organometallic chemistry, we often see one or two cyclopentadienyl ligands surrounding a metal atom, and forming the ubiquitous  $\text{CpML}_n$  and  $\text{Cp}_2\text{ML}_n$  complexes. The size and electronic properties of the Cp anion are just right for stabilizing these metal complexes. The usefulness of Cp is by no means limited to *d*-transition metal chemistry, but it has aided recent development of organoactinide chemistry as well [1–3]. Besides the familiar  $\text{CpML}_n$  and  $\text{Cp}_2\text{ML}_n$  stoichiometries, actinides frequently accommodate three Cp's at a metal center with an associated set of ligands, one or two in number. These are the  $\text{Cp}_3\text{ML}_n$  complexes ( $M = \text{Th}, \text{U}$ ), and  $\text{Cp}_3\text{UL}$  is the subject of this theoretical study.

The majority of the known  $\text{Cp}_3\text{ML}$  complexes contain monodentate anionic ligands such as halogens and alkyls.  $M$  is typically  $\text{U}^{\text{IV}}$ . The molecules possess trigonal-pyramidal or pseudo-tetrahedral geometry **1**, and dozens of X-ray structures give us a good picture of this class [4–10]. More rarely, neutral donors are bound to  $\text{Cp}_3\text{U}$ , giving unusual  $\text{U}^{\text{III}}$  complexes of the type  $\text{Cp}_3\text{UL}$  [11,12]. An interesting facet of the  $\text{Cp}_3\text{U}$  fragment is that  $\eta^2$ -acyl [13],  $\eta^2$ -pyrazolate [14], and even  $\eta^5$ -cyclopentadienyl [15] can be bound to it, despite apparent steric congestion of the

---

\* Dedicated to Professor Sei Otsuka, a pioneer in modern organometallic chemistry, on the occasion of his 65th birthday.

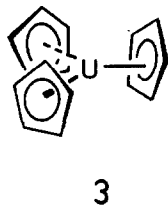


coordination sphere. With one more ligand, Cp<sub>3</sub>UL<sub>2</sub>, have been shown to exhibit trigonal-bipyramidal geometry **2**, where two L's occupy the axial positions [16,17].

In the present article we describe the basic features of the electronic structure of Cp<sub>3</sub>UL complexes, their geometry, and some aspects of bonding between U and ligands. Our study will then be extended to some specific topics, i.e.,  $\sigma$  and  $\pi$  bonding capabilities of uranium with ligands and a possibility of U-L multiple bonds. The analysis relies on molecular orbital calculations of the extended Huckel type with parameters detailed in Appendix.

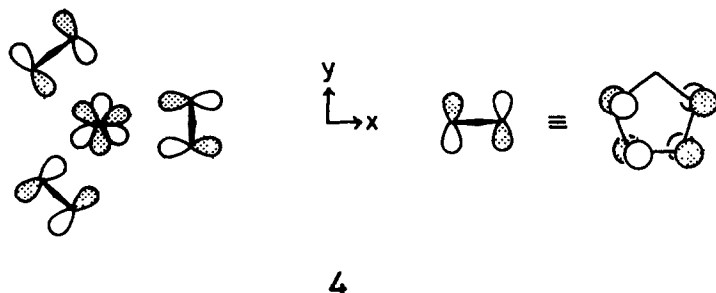
### The tris( $\eta^5$ -cyclopentadienyl)uranium fragment

Figure 1 shows a molecular orbital scheme for the tris( $\eta^5$ -cyclopentadienyl)uranium fragment of the pseudotrigonal planar geometry. The orientation of three Cp rings is chosen to be **3** with the molecular symmetry of  $C_{3v}$ . At right of the



figure, the U atom carries  $5f$ ,  $6d$ ,  $7s$ , and  $7p$  valence orbitals. Our calculations contain the inner  $6p$  orbitals having the energy of  $-30.03$  eV, but they are not shown in the figure. On the left, there are 15 frontier  $\pi$  orbitals resulting from three Cp ligands.

In the  $C_{3v}$  point group, two ligand orbitals have  $a_2$  symmetry, which can overlap only with a uranium  $f$  orbital,  $f_{y(3x^2-y^2)}$ . The lower occupied  $a_2$  in the  $\pi_2$  set interacts



with  $f_{V(3\lambda^2-1^2)}$  more strongly than the higher  $a_2$  in the vacant  $\pi_3^*$  nest, and the net outcome is destabilization of  $f_{V(3\lambda^2-1^2)}$ . **4** depicts the  $a_2(\pi_2)-f_{V(3\lambda^2-1^2)}$  bonding molecular orbital. Presence of  $f$ -orbital participation in bonding, to one degree or another, has occasionally been claimed in describing structures and chemical characteristic of lanthanide and actinide complexes [18–23]. For the  $Cp_3M$  complexes, the bonding interaction of  $a_2$  symmetry, **4**, occurs only when the metal contains valence  $f$  orbitals. This symmetry requirement, in conjunction with the fact that the bulk of the  $Cp_3M$  complexes are within the  $f$ -transition metal series, might imply the

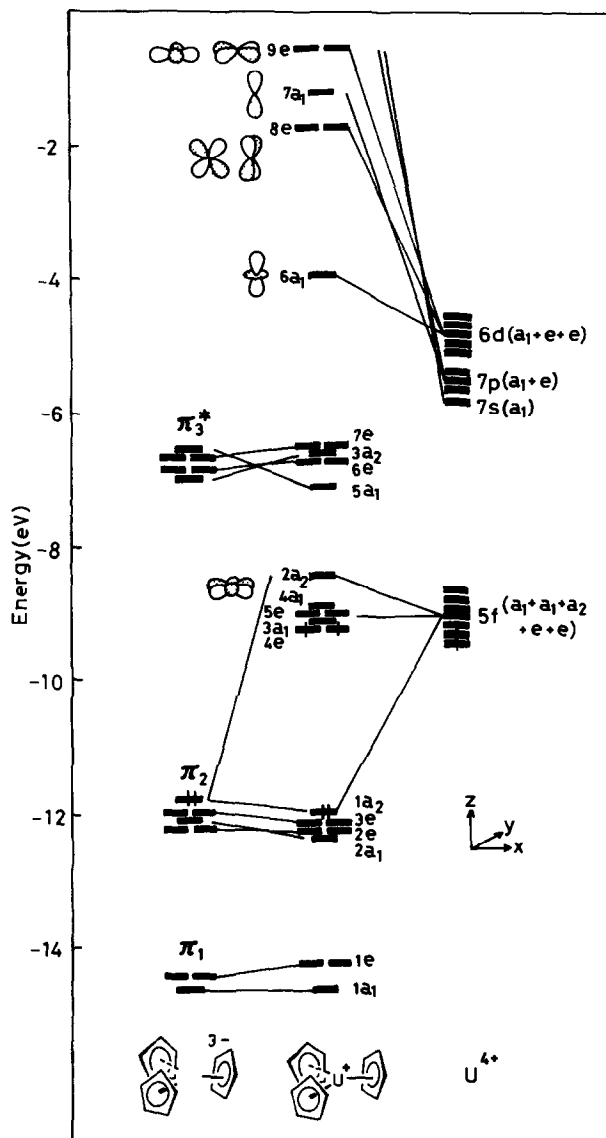


Fig. 1. Interaction diagram for the pseudo-trigonal-planar  $Cp_3U^+$  fragment. The molecular symmetry is  $C_{3v}$ .

importance of  $f$  orbitals in stabilizing the M–Cp bonds. However, the degree of U  $f$  admixture in the bonding  $1a_2$  molecular orbital is not great, amounting to 8% in our calculations. The rest of U  $f$  orbitals, having  $a_1$  or  $e$  symmetry, remain essentially non-bonding.

The U  $6d$ ,  $7s$ , and  $7p$  orbitals all move up in energy through interactions with Cp  $\pi$  orbitals by different amounts. Of these levels,  $s$ ,  $p_x$ , and  $p_y$  are strongly destabilized and are outside the energy range of Fig. 1. At somewhat lower energy, there are two degenerate  $e$  sets of  $d_{xz} + d_{yz}$  and  $d_{yz-1z} + d_{xz}$  character ( $8e$  and  $9e$ ), and  $7a_1$  with  $p_z$  character. At still lower energy,  $6a_1$  orbital consists mainly of  $d_{z^2}$  with 12%  $s$  admixture.

The  $Cp_3U$  complexes are made of the pyramidalized  $Cp_3U$  fragment, and we wish to know how the  $Cp_3U$  orbitals vary their energy levels as a function of  $\theta$ , the angle between the  $z$  axis and the normals to the Cp rings, 5. In the motion which



5

lowers  $\theta$  from  $90^\circ$ , the  $C_{3v}$  molecular symmetry is retained. Figure 2 plots the energy changes of the frontier orbitals. We are interested in the bonding capability of  $Cp_3U$  with ligands, so only the molecular orbitals which comprise primarily the uranium orbitals are shown in the figure.

The basic trend noted in the figure is that the orbitals made of U  $d$  are stabilized with pyramidalization and the one made of  $p_z$  is destabilized. One reason for this trend is an increased  $p$ – $d$  mixing as the fragment departs from the  $\theta = 90^\circ$  geometry. The effect is particularly evident for the  $6a_1$ – $7a_1$  pair. As a consequence of the mixing,  $p_z$ – $d_{z^2}$  (plus  $s$ ) mixing in this case, they repel each other. Thus the higher orbital  $7a_1$  goes up in energy while the lower one  $6a_1$  moves down. The  $6a_1$  hybrid directs along the  $z$  axis away from the three Cp ligands, and prepares itself for the interaction with an incoming ligand. Stabilization of  $8e$  ( $d_{xz} + d_{yz}$ ) with decreasing  $\theta$  comes from mixing with  $p_x + p_y$ . The  $9e$  set lacks ability to strongly hybridize with any  $p$  orbitals in the  $C_{3v}$  pyramidal structure, resulting in a slight downward curve. On the other hand, the U  $f$  orbitals stay approximately constant in energy.

Before going into interactions of the  $Cp_3U$  fragment with various ligands, we briefly comment on the nature of U–Cp bonds. As Fig. 1 shows, U  $6d$ ,  $7s$ , and  $7p$  are pushed up due to the interactions with Cp  $\pi$  orbitals. Nevertheless these uranium orbitals scarcely mix in the occupied Cp  $\pi_2$  orbitals, e.g. 3% in  $3e$  and  $2e$ , and 6% in  $2a_1$ . We have mentioned that  $f$ -orbital participation was also not great, 8% in  $1a_2$ . Therefore, the calculated U– $C_s$ (Cp) overlap population of the Mulliken type is fairly small, amounting to 0.05 for  $\theta = 90^\circ$ . When the hydrogen atoms of Cp are included, the overall U–Cp overlap population is reduced to 0.01. This contrasts with the large M–Cp overlap populations, 0.57, obtained for a typical  $d$  transition metal Cp complex  $CpFe(CH_3)(CO)_2$  [24]. From the small U–Cp overlap population, we deduce that the U–Cp bond has very weak covalent character, much weaker than the Fe–Cp bond in  $CpFe(CH_3)(CO)_2$ . The lack of covalency in the U–Cp  $\pi$

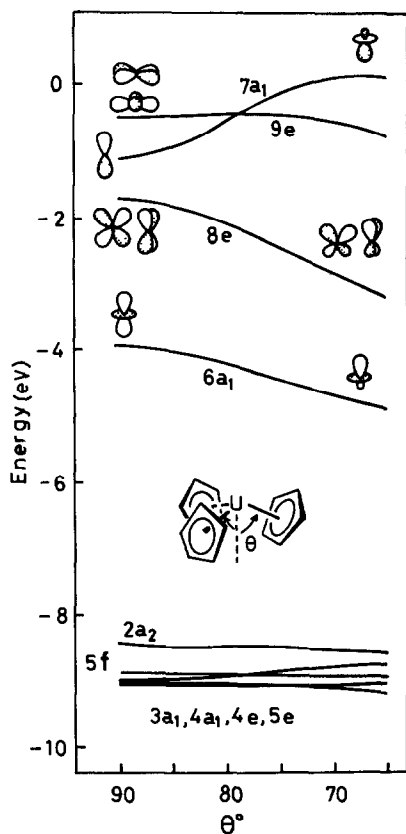


Fig. 2. Cp<sub>3</sub>U orbitals as a function of the pyramidal angle  $\theta$ . The molecular orbitals which comprise primarily uranium orbitals are shown in this diagram.

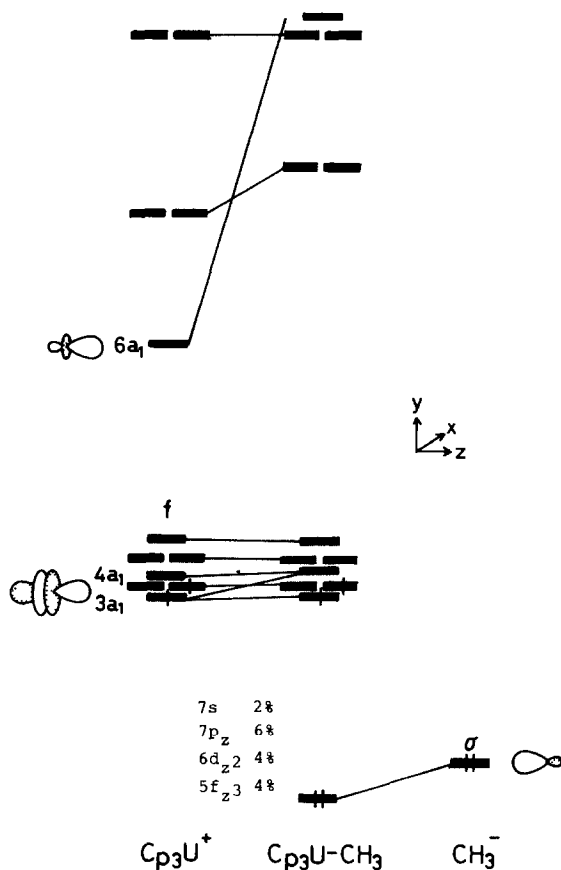
bond can be linked to the fact that  $\pi$  coordinations to actinides have so far been limited to anionic  $\pi$  ligands [4–10,21,25–26]. There are no actinide compounds with neutral ligands such as olefins and dienes etc., which are ubiquitous among  $d$  transition metal complexes. A single exception is the intriguing  $\pi$  arene complex of U<sup>III</sup>, U(AlCl<sub>4</sub>)<sub>3</sub>(C<sub>6</sub>H<sub>6</sub>). The molecule has rather long U–arene bond (U–C 2.91 Å), and even its existence is somewhat surprising [27].

### Interactions between the pyramidalized Cp<sub>3</sub>U and ligands

There are a good number of Cp<sub>3</sub>UL complexes with a variety of ligands L. Aside from Cp<sub>4</sub>U, the (Cp centroid)–U–(Cp centroid) angles open up from the ideal tetrahedral angle 109.47°, but only slightly, being typically 117°. The geometry may be termed a trigonally compressed tetrahedron. In our calculations on the Cp<sub>3</sub>UL complexes, we fixed the Cp–U–Cp angle to be 109° and did not take its minor opening-up effect into account. Other geometrical parameters are summarized in Appendix.

Let us first study the model complex Cp<sub>3</sub>UCH<sub>3</sub>. The methyl ligand is a simple type of ligand to consider, for it can bond practically in a pure  $\sigma$  manner. The

interactions between the  $\text{Cp}_3\text{U}$  unit and  $\text{CH}_3$  are given in **6**, where the energy levels are not drawn to scale. The methyl  $\sigma$  orbital overlaps very well with the fragment orbital  $6a_1$ , and somewhat with  $3a_1$  and  $4a_1$ . The latter two fragment orbitals both have  $f_z$  character, and their interactions with the methyl  $\sigma$  are in practice due to the  $f_z$ - $\sigma$  overlap. We have thus a reasonably strong  $\sigma$  bond between uranium and methyl. The presence of covalency in the bond is corroborated by the large  $\text{U}-\text{C}(\text{CH}_3)$  overlap population of 0.40. It is as large as the one (0.44) obtained for the  $\text{Fe}-\text{C}(\text{CH}_3)$  bond in  $\text{CpFe}(\text{CH}_3)(\text{CO})_2$ , and contrasts with the very small  $\text{U}-\text{Cp}$  overlap population. The formation of strong  $\text{U}-\text{C}(\text{CH}_3)$   $\sigma$  bond is also manifested in the composition of the bonding molecular orbital shown in **6**. U  $7s$ ,  $7p_z$ ,  $6d_{z^2}$ , and



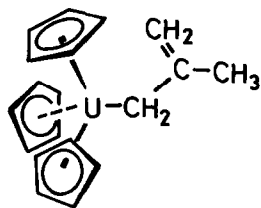
### 6

$5f_z$ , all contribute to the  $\sigma$  bond. Each contribution is small, but the total of them amounts to 16%.

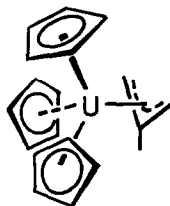
Structures of the  $\text{Cp}_3\text{ML}$  complexes have been summarized by Raymond and Eigenbrot, Jr., [28] who presented an explanation for the observed metal-to-carbon(Cp) distances based on the ionic radii of the metal ion and the Cp anion. For the  $\text{U}-\text{C}(\text{alkyl})$  bonds, three X-ray structures provide information. The uranium-to-carbon(alkyl or  $\sigma$ -allyl) distances in  $\text{Cp}_3\text{U}(\text{n}-\text{C}_4\text{H}_9)$  [5],  $\text{Cp}_3\text{U}(\text{CH}_2\text{-}p\text{-CH}_3\text{C}_6\text{H}_4)$  [5],

and  $\text{Cp}_3\text{U}[\sigma\text{-(CH}_2\text{)C(CH}_3\text{)CH}_2\text{}]$  [6] are 2.43, 2.54, and 2.48 Å, respectively. These bond lengths are obviously shorter than those of the U–C(Cp) distances which range from 2.71 to 2.74 Å in the molecules. Closely related to  $\text{Cp}_3\text{UR}$  include  $\text{Cp}_3\text{U}(\text{C}\equiv\text{CH})$  [7],  $\text{Cp}_3\text{U}(\text{C}\equiv\text{CC}_6\text{H}_5)$  [8], and  $\text{Cp}_3\text{UCHP}(\text{C}_6\text{H}_5)(\text{CH}_3)_2$  [10], all of which have been studied by X-ray analyses. An interesting aspect of these three complexes is that they involve shorter uranium-to-carbon distances compared with the aforementioned alkyl complexes, being 2.36, 2.33, and 2.29 Å, respectively. Shortening of the U–C bonds will be addressed to their partial multiple bond character in the following section.

We now turn to  $\text{Cp}_3\text{U}$  complexes with cyclopentadienyl and allyl. Unlike alkyls, these ligands have multicoordination mode possibilities depending on the metal fragments with which they interact. The X-ray structure analysis of  $\text{Cp}_3\text{U}[\text{CH}_2\text{C(CH}_3\text{)CH}_2]$  shows that the 2-methylallyl group is bound to uranium in a  $\eta^1$ -manner, **7** [29].

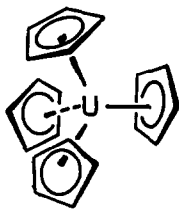


7

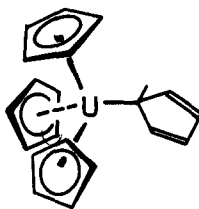


8

An alternative coordination mode, i.e. the  $\pi$ -allyl  $\eta^3$ -structure **8**, seems to be less stable. The steric reasoning cannot be applied to the geometrical choice, because in  $\text{Cp}_4\text{U}$  all rings are  $\eta^5$ . The Cp ring is bulkier than the allyl group, and yet favors the  $\eta^5$ -structure, **9** over  $\eta^1$ , **10**. Of the *d*-transition metal analogues,  $\text{Cp}_4\text{Zr}$  consists of



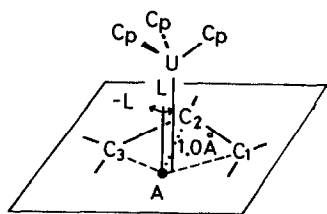
9



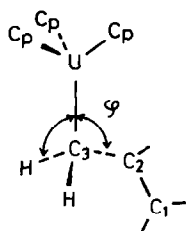
10

three  $\eta^5$ -Cp ligands and one  $\eta^1$ -Cp ligand, while  $\text{Cp}_4\text{Ti}$  and  $\text{Cp}_4\text{Hf}$  have two  $\eta^5$ -Cp's and two  $\eta^1$ -Cp's [30–34]. On an NMR time scale the molecules are fluxional with all four rings equivalent [35,36].

We have calculated two potential energy curves for  $\text{Cp}_3\text{U}[(\text{CH}_2)_2\text{CH}]$ , in an attempt to compare energies of its  $\eta^1$  (**7**) and  $\eta^3$  (**8**) structures. First consider the passage of the  $\text{Cp}_3\text{U}$  fragment across the face of an allyl molecule, moving as indicated in **11**. When  $\text{Cp}_3\text{U}$  is at right above the point A ( $L = 0$ ), the allyl complex assumes an ideal  $\pi$ -allyl  $\eta^3$ -structure. From there,  $\text{Cp}_3\text{U}$  is allowed to slip sideways toward the point above either  $\text{C}_1$  or  $\text{C}_3$ , keeping the U–allyl separation of 2.5 Å unchanged. The total energy profile for this movement is given by a solid curve at



11



12

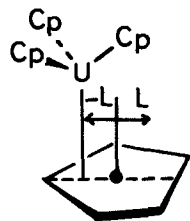
left of Fig. 3. Then the allyl group is pyramidalized at the  $C_3$  carbon, at above which  $Cp_3U$  resides ( $L = -1.25 \text{ \AA}$ ). The dashed line in Fig. 3 left describes energetics of this pyramidalization. The energy minimum appears at  $\varphi \approx 110^\circ$ , corresponding to a stable  $\eta^1$ -structure. Comparing energies of the two minima, one can see that the  $\eta^1$ -structure is indeed more stable than the  $\eta^3$ -structure. The energy difference was calculated to be  $0.40 \text{ eV}$  ( $9.2 \text{ kcal mol}^{-1}$ ). The  $^1\text{H}$  NMR spectrum of  $Cp_3U[(CH_2)_2CH]$  at  $179 \text{ K}$  has shown the  $A_2BCD$  pattern, characteristic of an  $\eta^1$ -allyl linkage. When the temperature goes up, the allyl group becomes fluxional through a  $\sigma \rightleftharpoons \pi \rightleftharpoons \sigma$  interconversion as **13** [37]. The barrier to the 1,3-migration of



13

$Cp_3U$  was estimated to be  $8\text{--}9 \text{ kcal mol}^{-1}$ , which accords quite well with our calculations in that a  $\pi$ -bonded  $\eta^3$ -intermediate lies  $9.2 \text{ kcal mol}^{-1}$  higher in energy than a  $\sigma$ -bonded  $\eta^1$ -structure.

We compare energies of  $(\eta^5\text{-Cp})_3(\eta^1\text{-Cp})U$  in Fig. 3 right. The solid curve shows the total energy change for  $Cp_3U$  passing in a plane  $2.55 \text{ \AA}$  above the Cp ring as defined in **14**. The energy minimum at  $L = 0 \text{ \AA}$  is for a geometry corresponding to



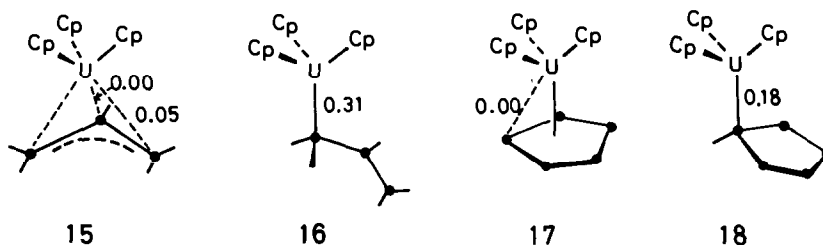
14

the  $(\eta^5\text{-Cp})_4U$  complex. Optimization of an  $\eta^1$ -structure is performed again by pyramidalizing the Cp ring at a  $\sigma$ -coordination site. Its energy profile is give by the dashed line which has a minimum at  $\varphi \approx 110^\circ$ . In contrast to the allyl case, the minimum is higher in energy than the minimum for  $Cp_4U$ . Thus the  $\eta^5$ -site of Cp is



where one better comes up with maximum stabilization for the  $\text{Cp}_3\text{U}$  fragment, as is experimentally observed in the X-ray structure.

Orbital symmetry arguments do not explain why  $\text{Cp}_3\text{U}(\text{allyl})$  and  $\text{Cp}_4\text{U}$  choose the structures that they have. Instead, the geometrical contrast between the molecules is a consequence of delicate energy balance. In this respect, the good agreement between our calculations and the experimentally observed structures may be fortuitous, and yet there is a reason for it. The argument runs as follows. The overlap populations calculated for U–C bonds in the  $\pi$ - and  $\sigma$ -structures of  $\text{Cp}_3\text{U}[(\text{CH}_2)_2\text{CH}]$  and  $\text{Cp}_4\text{U}$  are summarized in **15–18**. Comparing the two  $\pi$ -bonded structures, one



finds that the sum of U–C overlap populations in **15** is somewhat larger than that in **17**. Thus the covalent interactions can be stronger for the  $\pi$ -allyl complex. We think that the  $\pi$ -allyl structure itself is satisfactory, as far as bonding between U and the allyl part is concerned. Inspection of the orbital interactions shows that the filled NBMO of allyl anion finds a good overlap with one of the vacant  $\text{Cp}_3\text{U}$  8e orbitals and overlaps with the vacant  $f_{x^2-z^2}$  to some degree. These interactions are sketched in **19a** and **19b**, where the numbers denote the computed group overlap integrals. The outcome is the positive U–C (terminal) overlap population of 0.05. Then the

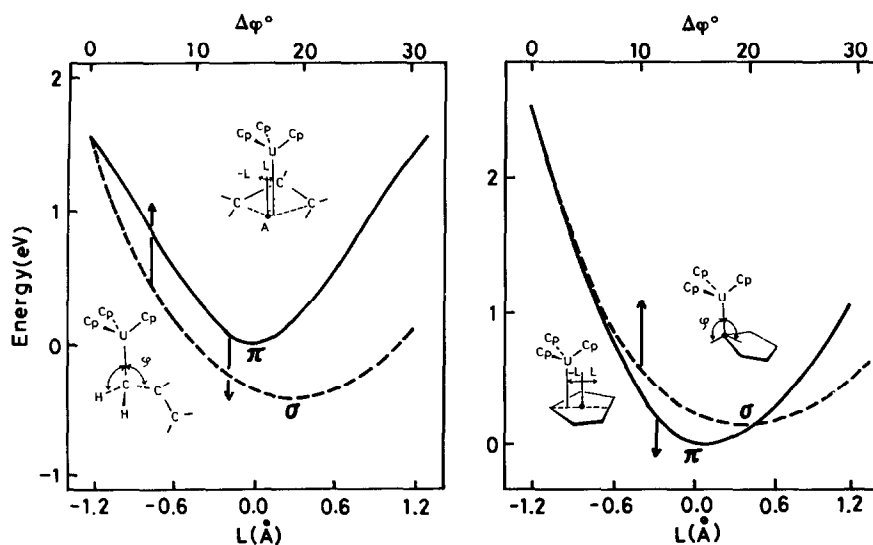
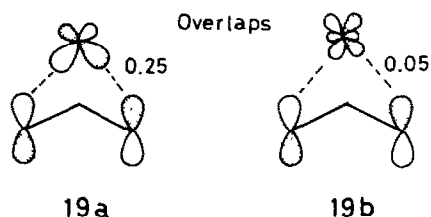
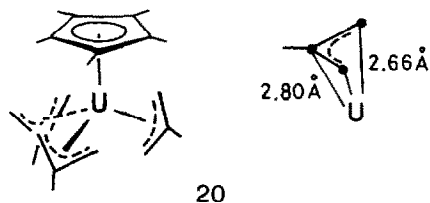


Fig. 3. Computed total energies for  $\text{Cp}_3\text{U}^+$  moving across the face of an allyl (left, solid curve) and of a cyclopentadienyl (right, solid curve). The dashed curves are those for pyramidalization at a terminal carbon of allyl (left) and at a cyclopentadienyl carbon (right), where  $\varphi = 90 + \Delta\varphi$ . The marks, “ $\pi$ ” and “ $\sigma$ ”, denote energy minima of  $\pi$ - and  $\sigma$ -structures of  $\text{Cp}_3\text{U}(\text{allyl})$  and  $\text{Cp}_4\text{U}$ .



difference in  $\sigma$ -bond strength between **16** and **18** should account for the geometrical contrast between  $\text{Cp}_3\text{U}(\sigma\text{-allyl})$  and  $(\eta^5\text{-Cp})_4\text{U}$ . The  $\text{U}-\text{C}(\sigma\text{-allyl})$  overlap population is substantially larger than the  $\text{U}-\text{C}(\sigma\text{-Cp})$  overlap population, indicating that allyl is a stronger  $\sigma$ -donor than Cp when coordinated to  $\text{Cp}_3\text{U}$ . The  $\text{U}-\text{C}(\sigma\text{-allyl})$  bond seems to be sufficiently strong to let the molecule choose the  $\eta^1$ -structure, while the  $\text{U}-\text{C}(\sigma\text{-Cp})$  bond is not strong enough to do so. The electron distribution in the free pyramidalized allyl and Cp anions corroborates the above trend. Negative charge ( $Q$ ) of allyl anion is very well localized to the carbon atom at which U coordination occurs ( $Q = -0.74e$ ). To the contrary, accumulation of negative charge at the coordination site is less pronounced ( $Q = -0.32e$ ) in  $\text{Cp}^-$ , indicating a weak  $\sigma$ -donor character of the  $\eta^1$ -Cp ligand.

An interesting compound recently investigated is  $(\text{C}_5\text{Me}_5)\text{U}[(\text{CH}_2)_2\text{CCH}_3]_3$ , which has the structure shown in **20** [38]. This is the first well-characterized actinide



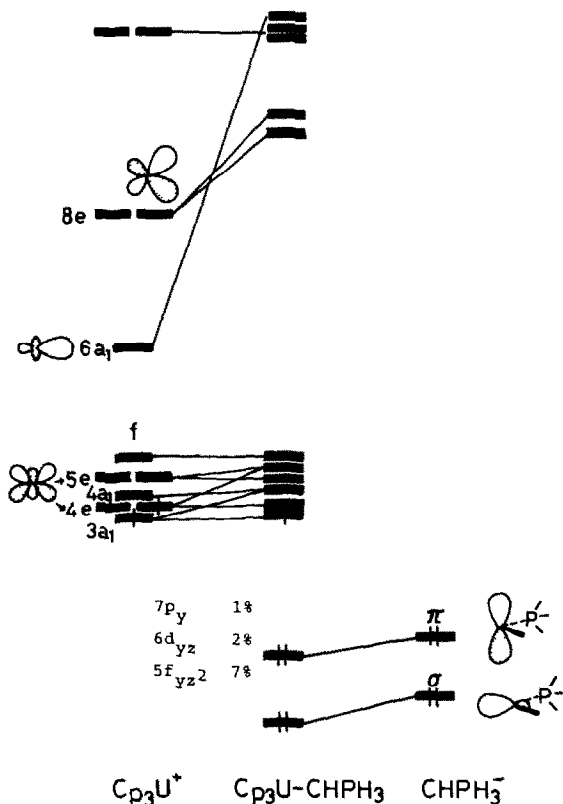
complex with  $\eta^3$ -allyl ligands, while the synthesis of  $\text{U}(\eta^3\text{-C}_3\text{H}_5)_4$  was briefly reported in as early as 1969 [39]. Perhaps most intriguing is the long  $\text{U}-\text{C}(\text{central})$  distance of 2.80 Å as compared with the average  $\text{U}-\text{C}(\text{terminal})$  distance of 2.66 Å. The overlap populations calculated for  $\text{Cp}_3\text{U}(\eta^3\text{-allyl})$  (**15**) shows a similar trend, i.e., less involvement of the central carbon in  $\text{U}$ -allyl bonding. It should be noted that the allyl central carbon is generally closest to a  $d$ -transition metal [40], except for the  $d^1$   $\text{Cp}_2\text{Ti}(\eta^3\text{-2,3-dimethylallyl})$  complex [41].

### Possibilities of uranium-carbon multiple bonds

In the preceding section, we briefly mentioned that  $\text{U}-\text{C}(\text{L})$  distances in  $\text{Cp}_3\text{UL}$  ( $\text{L} = \text{alkyls, acetylides, etc.}$ ) are diverse. They range from 2.29 in  $\text{Cp}_3\text{UHP}(\text{C}_6\text{H}_5)(\text{CH}_3)_2$  to 2.54 Å in  $\text{Cp}_3\text{U}(\text{CH}_2\text{-}p\text{-CH}_3\text{C}_6\text{H}_4)$ , the former of which is the shortest  $\text{U}-\text{C}$  distance known so far. In the related phosphoylide complex,  $\text{CpU}[(\text{CH}_2)(\text{CH}_2)\text{P}(\text{C}_6\text{H}_5)_2]_3$ , the  $\text{U}-\text{C}$   $\sigma$  bond is as long as 2.66 Å [42]. The variation of distances is not simply related to steric crowding or ligand-ligand repulsion, because the complexes are all crowded molecules. Instead the root for the observed trend can be looked for in the nature of bonds, e.g. differences in covalent bond strengths. We here focus our attention on the short  $\text{U}-\text{C}$  distances in

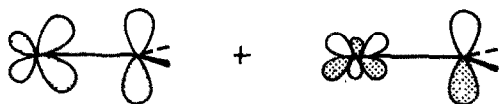
$\text{Cp}_3\text{U}(\text{C}\equiv\text{CR})$  and  $\text{Cp}_3\text{UChp}(\text{C}_6\text{H}_5)(\text{CH}_3)_2$ . It will be shown that presence of U–C multiple bond character is responsible for the bond shortening.

Consider a model  $\text{Cp}_3\text{UChp}(\text{C}_6\text{H}_5)(\text{CH}_3)_2$ . The calculations were done using the observed U–C distance (2.29 Å) in  $\text{Cp}_3\text{UChp}(\text{C}_6\text{H}_5)(\text{CH}_3)_2$ . The  $\text{Chp}(\text{C}_6\text{H}_5)(\text{CH}_3)_2$  ligand carries a  $\pi(\text{C } p_y)$  orbital in addition to the  $\sigma$  lone-pair orbital as shown in the interaction diagram 21. The  $\sigma$  orbital overlaps with the  $\text{Cp}_3\text{U } 6a_1, 3a_1$  and  $4a_1$ , forming a U–C



21

$\sigma$  bond. This is quite similar to the U– $\text{CH}_3$  interaction given in 6. Then another interaction comes in. The  $\pi$  orbital, being perpendicular to the  $\sigma$ , is nearly pure  $\text{C } p_y$ , and interacts well with  $\text{Cp}_3\text{U } 8e$  and  $f_{yz^2}$ . As a result,  $\text{Chp}_3^-$  is stabilized and now contains contribution from the U  $p_y$  (1%),  $d_{yz}$  (2%), and  $f_{yz^2}$  (7%) orbitals. The calculated U–C overlap population amounts to 0.61, where the  $\pi$  interaction 22



22

contributes 0.19 to it. Recall that the U– $\text{C}(\text{CH}_3)$  overlap population was 0.40, which

was calculated for  $\text{Cp}_3\text{U}\text{CH}_3$  assuming the U–C distance of 2.4 Å. The large overlap population for  $\text{Cp}_3\text{U}\text{CHPH}_3$  is not a result of our choice of the short, 2.29 Å, U–C bond in the model compound. Calculations on  $\text{Cp}_3\text{U}\text{CHPH}_3$  with distance of 2.4 Å reduces the overlap population only slightly to 0.57 (0.15 from the  $\pi$  interaction). It is still substantially larger than the one for U–C( $\text{CH}_3$ ). The idea of U–C multiple bond character thus gains support from our theoretical analysis [10,13,43].

The  $\text{CHP}(\text{C}_6\text{H}_5)(\text{CH}_3)_2^+$  ligand is electronically analogous to carbenes. One may categorize the numerous transition metal carbene complexes into the two classes; the Fischer type with electrophilic carbenes [44] and the Schrock type with nucleophilic carbenes [45]. Calculations on the model  $\text{Cp}_3\text{U}\text{CHPH}_3$  place a highly negative charge of  $-1.38$  on the ylide carbon and an electron population of 1.71 in the C  $p_y$  orbital. Nucleophilicity of the “ylide carbene” in  $\text{Cp}_3\text{U}\text{CHPH}_3$  is evident. Probably its nucleophilic character is even stronger than Schrock type carbenes. Such a feature arises from the trend that uranium valence orbitals are high in energy and the C  $p_y$  orbital of  $\text{CHPH}_3$  stays much lower than those.

It has been suggested that the short U–C distances in  $\text{Cp}_3\text{U}(\text{C}\equiv\text{CR})$  might reflect multiple metal carbon bonds [29]. Our calculations on  $\text{Cp}_3\text{U}(\text{C}\equiv\text{CH})$ , with U–C distance of 2.4 Å, confirm this view. The computed U–C overlap population is 0.60, which is again much larger than the U–C( $\text{CH}_3$ ) overlap population. However, the contribution from U–C  $\pi$  interactions (0.10) is smaller than the one obtained for  $\text{Cp}_3\text{U}\text{CHPH}_3$ . The degree of U–C multiple bond character in  $\text{Cp}_3\text{U}(\text{C}\equiv\text{CH})$  appears to be less pronounced than one might expect from the fact that the cylindrical U–C( $\text{C}\equiv\text{CH}$ ) bond involves potentially two  $\pi$  interactions, perpendicular to each other.

## Appendix

The extended Hückel parameters are listed in Table 1 [46]. Exponents of the Slater-type uranium orbitals were estimated from the relativistic Dirac-Fock wave functions of Desclaux [47]. The U  $7s$  and  $7p$  orbitals are of single- $\zeta$  type, exponents of which were determined from  $R_{\text{max}}$ , radius of maximum radial density, of the U  $7s_{1/2}$  function. For the double- $\zeta$  parameters of U  $6d$  and  $5f$ , we used  $R_{\text{max}}$ ,  $\langle r \rangle$ , and  $\langle r^2 \rangle$  of U  $6d_{5/2}$  and  $6d_{3/2}$ , and those of U  $5f_{7/2}$  and  $5f_{5/2}$ , respectively.  $H_{ii}$  values

TABLE 1  
EXTENDED HÜCKEL PARAMETERS

Orbital	$H_{ii}$ (eV)	Exponent
U $7s$	–5.50	1.914
$7p$	–5.50	1.914
$6d$	–5.09	2.581 (0.7608) + 1.207(0.4126)
$5f$	–9.01	4.943(0.7844) + 2.106(0.3908)
$6p$	–30.03	4.033
P $3s$	–18.6	1.60
$3p$	–14.0	1.60
C $2s$	–21.4	1.625
$2p$	–11.4	1.625
H $1s$	–13.6	1.3

were also taken from the Desclaux's functions. In transforming the relativistic functions of U *6d*, *5f*, and *6p* to non-relativistic ones, we took weighted averages of each multiplets. The parameters for the other elements are standard ones. The off-diagonal elements  $H_{ij}$  were calculated by a weighted Wolfsberg-Helmholtz formula with the standard *K* value of 1.75.

$$H_{ij} = K \frac{S_{ij}}{2} [(1 + \Delta) H_{ii} + (1 - \Delta) H_{jj}]$$

$$\text{where } \Delta = \frac{H_{ii} - H_{jj}}{H_{ii} + H_{jj}}$$

Geometrical assumptions included the following: Cp<sub>2</sub>U-CH<sub>3</sub>; U-Cp(centroid) 2.54, C-C(Cp) 1.42, U-C(CH<sub>3</sub>) 2.40, C-H 1.09 Å, Cp(centroid)-U-Cp(centroid) 109°; Cp<sup>3</sup>U[(CH<sub>2</sub>)<sub>2</sub>CH]; C-C(allyl) 1.40 Å, C-C-C(allyl) 120°; Cp<sub>4</sub>U; U-Cp(centroid) 2.55 Å, Cp(centroid)-U-Cp(centroid) 109.47°; Cp<sub>3</sub>U-CHPH<sub>3</sub>; U-C 2.29, C-P 1.69, P-H 1.42 Å, U-C-P 142°, U-C-H 98°; Cp<sub>3</sub>U(C≡CH); U-C 1.40, C≡C 1.25, C-H 1.09 Å.

## References

- 1 T.J. Marks, *Science*, 217 (1982) 989, and refs. therein.
- 2 T.J. Marks, *Prog. Inorg. Chem.*, 25 (1979) 223.
- 3 T.J. Marks, J.M. Manriquez, P.J. Fagan, V.W. Day, C.S. Day, and S.H. Vollmer, *ACS Symposium Series*, 131 (1980) 1.
- 4 (a) C. Wong, T. Yen, and T. Lee, *Acta Crystallogr.*, 18 (1965) 340; (b) R.R. Ryan, R.A. Penneman, and B. Kanellakopoulos, *J. Am. Chem. Soc.*, 97 (1975) 4258; (c) J.H. Burns and P.G. Laubereau, *Inorg. Chem.*, 10 (1971) 2798; (d) J. Leong, K.O. Hodgson, and K.N. Raymond, *Inorg. Chem.*, 12 (1973) 1329.
- 5 G. Parego, M. Cesari, F. Farina, and G. Lugli, *Acta Crystallogr.*, B, 32 (1976) 3034.
- 6 G.W. Halstead, E.C. Baker, and K.N. Raymond, *J. Am. Chem. Soc.*, 97 (1975) 3049.
- 7 M. Tsutsui, N. Ely, and R. Dubois, *Acc. Chem. Res.*, 9 (1976) 217.
- 8 J.L. Atwood, C.F. Hains, M. Tsutsui, and A.E. Gebala, *J. Chem. Soc., Chem. Commun.*, (1973) 452.
- 9 J.L. Atwood, M. Tsutsui, N. Ely, and A.E. Gebala, *J. Coord. Chem.*, 5 (1976) 209.
- 10 R.E. Cramer, R.B. Maynard, J.C. Paw, and J.W. Gilje, *J. Am. Chem. Soc.*, 103 (1981) 3589.
- 11 (a) P. Zanella, G. Rossetto, G. De Paoli, and O. Traverso, *Inorg. Chim. Acta*, 44 (1980) L155; (b) B. Kanellakopoulos, E.O. Fischer, E. Dormberger, and F. Baumgärtner, *J. Organomet. Chem.*, 24 (1970) 507.
- 12 J.G. Brennan, R.A. Andersen, and A. Zalkin, *J. Am. Chem. Soc.*, submitted.
- 13 R.E. Cramer, R.B. Maynard, J.C. Paw, and J.W. Gilje, *Organometallics*, 1 (1982) 869.
- 14 C.W. Eigenbrot, Jr and K.N. Raymond, *Inorg. Chem.*, 20 (1981) 1553.
- 15 J.H. Burns, *J. Am. Chem. Soc.*, 95 (1973) 3815.
- 16 R.D. Fischer, E. Klähne, and J. Kopf, *Z. Naturforsch. B*, 33 (1978) 1393.
- 17 R.D. Fischer and G.R. Stenel, *J. Organomet. Chem.*, 156 (1978) 383.
- 18 C.A. Coulson and G.R. Lester, *J. Chem. Soc.*, (1956) 3650.
- 19 S.P. McGlynn and J.K. Smith, *J. Mol. Spectrosc.*, 6 (1961) 164.
- 20 L. Cattalini, U. Croatto, S. Degetto, E. Tondello, *Inorg. Chim. Acta Rev.*, 5 (1971) 19.
- 21 A. Streitwieser, U. Mueller-Westerhoff, G. Sonnichsen, D.G. Morell, K.O. Hodgson, and C.A. Harmon, *J. Am. Chem. Soc.*, 95 (1973) 8644.
- 22 M. Tsutsui, N. Ely, and A. Gebala, *Inorg. Chem.*, 14 (1975) 78.
- 23 (a) K. Tatsumi, K. Kasuga, and M. Tsutsui, *J. Am. Chem. Soc.*, 101 (1979) 484; (b) K. Tatsumi and M. Tsutsui, *ibid.*, 102 (1980) 882.
- 24 K. Tatsumi and R. Hoffmann, *Inorg. Chem.*, 23 (1984) 1633.
- 25 M.R. Spirlet, J. Rebizant, and J. Goffart, *Acta Crystallogr.*, B, 38 (1982) 2400.

- 26 E.A. Mintz, K.G. Maloy, T.J. Marks, and V.W. Day, *J. Am. Chem. Soc.*, 104 (1982) 4692.
- 27 M. Cesari, U. Pedretti, A. Zazetta, G. Lugli, and W. Marconi, *Inorg. Chim. Acta*, 5 (1971) 439.
- 28 K.N. Raymond and C.W. Eigenbrot, Jr. *Acc. Chem. Res.*, 13 (1980) 276.
- 29 G.W. Halstead, E.C. Baker, and K.N. Raymond, *J. Am. Chem. Soc.*, 97 (1975) 3049.
- 30 V.I. Kulishov, E.M. Brainina, N.G. Bokiy, and Yu.T. Struchkov, *J. Chem. Soc., Chem Commun.*, (1970) 475.
- 31 V.I. Kulishov, E.M. Brainina, N.G. Bokiy, and Yu.T. Struchkov, *J. Organomet. Chem.*, 36 (1972) 333.
- 32 J.L. Calderon, F.A. Cotton, B.G. DeBoer, and J. Takats, *J. Am. Chem. Soc.*, 93 (1971) 3592
- 33 R.D. Rogers, R.V. Bynum, and J.L. Atwood, *J. Am. Chem. Soc.*, 100 (1978) 5238.
- 34 R.D. Rogers, R.V. Bynum, and J.L. Atwood, *J. Am. Chem. Soc.*, 103 (1981) 692.
- 35 J.L. Calderon, F.A. Cotton, and J. Takats, *J. Am. Chem. Soc.*, 93 (1971) 3587
- 36 M.K. Minacheva, E.M. Brainina, and R.K. Freidlina, *Dokl. Akad. Nauk. SSSR*, 173 (1967) 581.
- 37 T.J. Marks, A.M. Seyam, and J.R. Kolb, *J. Am. Chem. Soc.*, 95 (1973) 5529.
- 38 T.H. Cymbaluk, R.D. Ernst, and V.W. Day, *Organometallics*, 2 (1983) 963
- 39 G. Lugli, W. Marconi, A. Mazzei, N. Paladino, and U. Pedretti, *Inorg. Chim. Acta*, 3(1969) 253.
- 40 D.J. Brauer and C. Kruger, *Organometallics*, 1(1982) 204, 207, and refs therein
- 41 R.B. Helmholtz, F. Jelinek, H.A. Martin, and A. Vos, *Recl. Trav. Chim. Pays-Bas*, 86 (1967) 1263.
- 42 R.E. Cramer, A.T. Mori, R.B. Maynard, J.W. Gilje, K. Tatsumi, and A. Nakamura, *J. Am. Chem. Soc.*, 106 (1984) in press.
- 43 R.E. Cramer, K.T. Higa, S.L. Pruskin, and J.W. Gilje, *J. Am. Chem. Soc.*, 105 (1983) 6749
- 44 E.O. Fischer, *Adv. Organomet. Chem.*, 14 (1976) 1, and refs. therein
- 45 R.R. Schrock, *Acc. Chem. Res.*, 12 (1979) 98, and refs. therein.
- 46 K. Tatsumi and R. Hoffmann, *Inorg. Chem.*, 19 (1980) 2656.
- 47 J.P. Desclaux, *At. Data Nucl. Data Tables*, 12 (1973) 311